Biogeosciences Discuss., doi:10.5194/bg-2016-49, 2016
Manuscript under review for journal Biogeosciences
Published: 17 February 2016

Biogeosciences Discussions
Open Access
EGU

Variations in triple isotope composition of dissolved oxygen and primary production in a subtropical reservoir

Hana Jurikova[1†], Tania Guha[1], Osamu Abe[2], Fuh-Kwo Shiah[1], Chung-Ho Wang[3], and Mao-Chang Liang[1,4,5,6]

[1]Research Center for Environmental Changes, Academia Sinica, 11529 Taipei, Taiwan
[2]Graduate School of Environmental Studies, Nagoya University, Chikusa, 464-8601 Nagoya, Japan
[3]Institute of Earth Sciences, Academia Sinica, 11529 Taipei, Taiwan
[4]Graduate Institute of Astronomy, National Central University, 32001 Jhongli, Taiwan
[5]Institute of Astronomy and Astrophysics, Academia Sinica, 11529 Taipei, Taiwan
[6]Department of Physics, University of Houston, Houston, TX 77004, USA
[†]Now at: GEOMAR Helmholtz-Zentrum für Ozeanforschung Kiel, Wischhofstr. 1-3, 24148 Kiel, Germany

Correspondence to: Mao-Chang Liang (mcl@rcec.sinica.edu.tw)

Abstract. Lakes and reservoirs play an important role in the carbon cycle, and therefore, monitoring their metabolic rates is essential. The triple oxygen isotope anomaly of dissolved O_2 [$^{17}\Delta = \ln(1+\delta^{17}O) - 0.518\times\ln(1+\delta^{18}O)$] offers a new, in situ, perspective on primary production, but is yet to be evaluated in freshwater systems. We investigated the $^{17}\Delta$ together with oxygen-argon ratio ($\delta O_2/Ar$) in the subtropical Feitsui Reservoir in Taiwan from June 2014 to July 2015. Here, we present the seasonal variations in $^{17}\Delta$, GP (gross production), NP (net production) and the NP/GP (net to gross ratio) in association with environmental parameters measured. The $^{17}\Delta$ varied with depth and season, with values ranging between 19 and 186 per meg. The $^{17}\Delta$ GP rates were lower from April to September averaging 215±93 mg C m^{-2} d^{-1} and higher from October to January averaging 523±66 mg C m^{-2} d^{-1}. The estimated average annual $^{17}\Delta$ GP was 104 g C m^{-2} $year^{-1}$ and the average annual NP was 22 g C m^{-2} $year^{-1}$. Overall, the NP/ GP varied slightly between 0.02 and 0.36 and the reservoir was net autotrophic in the mixed layer. Comparisons between $^{17}\Delta$ GP rates and the production rates estimated by in vitro ^{14}C bottle incubation method (^{14}C GP) were consistent on the same order of magnitude, with the $^{17}\Delta$ GP/^{14}C GP ratio of 1±0.8 throughout the study. Although typhoon occurrences were scarce, higher than average $^{17}\Delta$ values and $^{17}\Delta$ GP rates were recorded after typhoon events.

Key words. Triple oxygen isotope anomaly, ^{17} O-excess, oxygen-argon ratio, ^{14}C bottle incubations, carbon cycle, primary production, gross production, net production, freshwater system, Feitsui Reservoir

Biogeosciences Discuss., doi:10.5194/bg-2016-49, 2016
Manuscript under review for journal Biogeosciences
Published: 17 February 2016

1 Introduction

It is well established that marine photosynthesis plays a critical role in the global biogeochemical cycling of carbon and oxygen that sustain the great majority of ecosystems on our planet. Recent studies show that freshwater systems constitute a significant component of these cycles and deserve closer attention (Cole et al. 2007, Tranvik et al. 2009, Valdespino-Castillo et al. 2013). Assessing primary production (PP) and providing accurate estimates of ecosystems metabolic rates is therefore a key for understanding each system's fluxes and variability in biogeochemical cycling.

Traditionally, PP has been evaluated by in vitro ^{14}C bottle incubation method introduced by Steeman-Nielsen (1952). However, these measurements are associated with a number of biases and the interpretation of the PP estimates is problematic. The main drawback is the in vitro methodology, which involves the removal of plankton communities from the natural environment and confining it to a small volume of water, with variability in PP observed under laboratory conditions. Because the distribution of plankton is heterogeneous in time and space, these experiments can only provide local and instantaneous PP rates, which do not reflect the time-averaged mean PP rate. The PP rates observed in vitro therefore cannot be fully representative of natural PP rates (e.g. Harrison and Harris 1986, Marra 2002).

Over a decade and half ago, Luz et al. (1999) and Luz & Barkan (2000) introduced triple oxygen-isotopes or ^{17}O-excess ($^{17}\Delta$), which allows to assess PP in situ. The excess is defined as

$$^{17}\Delta = \ln(1+\delta^{17}O) - \lambda \times \ln(1+\delta^{18}O), \quad (1)$$

where the isotopic compositions $\delta^{17}O$ and $\delta^{18}O$ represent the deviation of the abundance ratio of an isotopic and normal species in a sample relative to that of a standard: $\delta^{*}O = ([^{*}O]/[^{16}O])_{sample}/([^{*}O]/[^{16}O])_{standard} - 1]$, $^{*}O$ is either ^{17}O or ^{18}O. Here, $\delta^{17}O$ and $\delta^{18}O$ are expressed with respect to atmospheric air O_2. Following Luz & Barkan (2005), the factor λ is taken to be 0.518. The basic premise of this method lies in the processes fractionating O_2 isotopologues. While photochemical reactions in the stratosphere (the coupled chemistry between O_2, O_3, and CO_2) give rise to non-mass-dependent signal in the atmospheric O_2 (Luz et al. 1999), respiration and photosynthesis fractionate O_2 in a mass-dependent way (the ^{17}O enrichment is approximately half of the ^{18}O relative to ^{16}O), which in a marine or aquatic systems allows for distinguishing the O_2 produced biologically from air O_2 entraining during gas exchange. Respiration modifies the dissolved O_2 concentrations in water but does not affect the $^{17}\Delta$, because the relative proportions of $\delta^{17}O$ and $\delta^{18}O$ remain the same. The respiratory effect on dissolved O_2 saturation can be evaluated using oxygen/argon ratios, expressed $\delta O_2/Ar$, because of the similar physical properties of O_2 and Ar, but no biological sources or sinks for Ar. Up-to-date this joint geochemical budget approach ($^{17}\Delta$ and $\delta O_2/Ar$) has been applied widely to study marine production in the Atlantic (Luz & Barkan 2009, Quay et al. 2012),

Biogeosciences Discuss., doi:10.5194/bg-2016-49, 2016
Manuscript under review for journal Biogeosciences
Published: 17 February 2016

Pacific (Hendricks et al. 2005, Sarma et al. 2005, 2006, 2008, Quay et al. 2010, Prokopenko et al. 2011, Stanley et al. 2010, Juranek et al 2010, 2012, Munro et al. 2013) and the Southern Ocean (Reuer et al. 2007, Hamme et al. 2012, Huang et al. 2012, Castro-Morales et al. 2013), yet other oceanic basins and freshwater systems in general remain by far and large unstudied.

In this study, we explore the applicability of the $^{17}\Delta$ method in an aquatic system. We use the $^{17}\Delta$ method to trace the photosynthetic O_2 fate and to investigate the seasonal changes in PP in a semi-closed subtropical reservoir over the period of one year and show that this approach may offer new perspectives on PP in lakes. In an effort to contribute to the understanding of production rates measured in situ using the $^{17}\Delta$ method and the in vitro estimates from the ^{14}C bottle incubation approach, and to expand this to freshwater systems, we provide thorough comparisons between the respective rates. In addition, we show data on the isotopic composition ($\delta^{18}O$, δ^{D}, and $^{17}\Delta$) of water from the reservoir. Understanding the isotopic composition of the Feitsui Reservoir water is crucial for accurate assessments of production rates using the $^{17}\Delta$ method and also offers insights into the biogeochemical/hydrological cycling of the reservoir. Ultimately, this paper presents a contribution to the studies on Feitsui Resevoir, a socio-economically and ecologically important freshwater reservoir.

2 Methods

2.1 Site description

The subtropical Feitsui Reservoir, located in northern Taiwan, is the country's second largest reservoir by volume (first is southern Tsengwen Dam), serving as the main water source for over five millions of people in the Taipei metropolitan area. The domestic demand is supplied by water releases from the Feitsui Reservoir and unregulated flow from Nanshin Creek downstream of the watershed. The upstream watershed encompasses the Beishi stream basin a branch of Xindian River, one of the three major tributaries of Tamsui River. The total catchment area of the reservoir is 303 km^2 and storage volume at normal maximum water level is 406 million m^3. The mean depth of the watershed is 40 m with maximum depth of 113 m near the dam site. The mean daily inflow to Feitsui Reservoir is ~30 m^3/s and the amount of water released depends on the reservoir's storage capacity and whether flow from Nanshin Creek is sufficient to supply domestic demand (Shiau & Wu 2010). The water residence time in the reservoir tends to be relatively long; in 2001 the average water residence time in the reservoir was 115 days (Chen et al. 2006). In the past the reservoir was found to alternate between mesotrophic and oligotrophic states (Kuo et al. 2003) although more recent studies (Kuo et al. 2006) observed a trend towards eutrophication. In 2012 according to Carlson's Trophic State Index (CTSI) the reservoir was in a mesotrophic state.

Biogeosciences Discuss., doi:10.5194/bg-2016-49, 2016
Manuscript under review for journal Biogeosciences
Published: 17 February 2016

In order to prevent deterioration of water quality the watershed is protected by Feitsui Reservoir Administration with restricted access to the water as well as adjacent area and any commercial and recreational activities prohibited. In addition, Feitsui Reservoir Administration operates a meteorological station, with wind speed among other parameters continuously monitored near the lake.

2.2 Water sampling and processing of samples

Sampling was carried out at station S1 (24.9 E, 121.566667 N, Figure 1) in the Feitsui Reservoir in the upper 100 m, located in the deepest region of the lake (~113 m). Water samples were collected on thirteen separate trips to the reservoir covering all seasons of the year from June 2014 to July 2015 using 5-L Niskin bottles with a manual messenger. Standard vertical profiles of conductivity, temperature and pressure were obtained routinely using Sea-Bird CTD equipped with additional sensors for fluorescence and dissolved oxygen measurements; accuracy was verified against in vitro measurements. A PAR sensor (BioTech) was used to measure photic irradiance.

Dissolved gasses were extracted from water following Emerson et al. (1995) and Luz et al. (2002). In summary, 300 flasks with LouwersHapert© O-ring stopcock, containing 50µl of saturated $HgCl_2$ solution, were evacuated prior to sampling and closed with a water lock. Approximately 150 mL of water sample was collected in the flask, leaving 150 mL of headspace for gases to exsolve. Once stopcock closed, the port was filled with the same water as sampled and sealed with a rubber cap to avoid air contamination. All samples were equilibrated for 24 h in a shaker at room temperature. After equilibration water was removed from the samples and the flasks were subsequently connected to a preparation system for removal of condensable gases including moisture at liquid nitrogen temperature. Extracted gases were then either stored in a sealed glass tubes or directly connected to a GC system (Thermo Scientific TRACE Gas Chromatograph) for complete removal of N_2 and other contaminates. The separation was done using a chromatographic column (3 m long, 1/8" SS tube, with molecular sieve 5A at mesh 60/100), modified from Barkan & Luz (2003). During separation the chromatographic column was kept at room temperature, and the yielded oxygen-argon mixture was absorbed onto two pellets of molecular sieve (1.6 mm, 5A, manufactured by SUPELCO) for subsequent isotopic analysis.

Water samples for δ^D and δ^{18} O analysis were collected in 15 ml centrifuged tubes and sealed with Parafilm M® to prevent from any isotopic alterations due to evaporation. Prior to analysis, water from the tubes was transferred to 2 ml vials with the aid of a pipette and analysed in a Picarro L2130-I Isotopic H_2O Analyser, following Laskar et al. (2014). δ^D and δ^{18} O values are expressed with respect to VSMOW (‰). The $^{17}\Delta$ of water was determined using CoF3 fluorination method following Barkan and Luz (2005). Briefly, 5 uL of water was converted to O_2 by injecting to CoF_3 reaction tube heated at 370°C under helium flow. The evolved oxygen gas was collected by a 13X molecular sieve U-trap at liquid nitrogen temperature, and

Biogeosciences Discuss., doi:10.5194/bg-2016-49, 2016
Manuscript under review for journal Biogeosciences
Published: 17 February 2016

then determined by dual-inlet mass spectrometry (Thermo Scientific Delta Plus). Mean standard deviations (1-σ) of multiple duplicate analyses for various waters (including VSMOW2, GISP, and SLAP) for $\delta^{17}O$, $\delta^{18}O$, and $^{17}\Delta$, were 0.086‰, 0.168‰, and 11 per meg, respectively. Each analysis (each sample) was measured in 80 sample-standard combinations.

Typhoon information was obtained from the Typhoon DataBase (http://rdc28.cwb.gov.tw/TDB/ctrl_typhoon_range_search). For visualization and analysis of profile data we have used Ocean Data View (ODV, Schlitzer 2015).

2.3 Stable isotope analysis of dissolved oxygen

$\delta^{17}O$ and $\delta^{18}O$ of O_2 in a purified oxygen-argon mixture were determined by dual inlet mass spectrometry (Thermo Scientific Finnigan MAT 253 Stable Isotope Ratio Mass Spectrometer). Each sample was run for 3 acquisitions, 12 cycles for each. The reported δ values are the average of 36 cycles. The analytical precision (1-σ standard error of the mean n=36 multiplied by Student's t-factor for a 95% confidence limits after two sigma outlier removal) for $\delta^{17}O$ and $\delta^{18}O$ is 0.013‰ and 0.006‰, respectively. Our long-term precision (1-σ standard deviation) of routine measurements of atmospheric air O_2 for $\delta^{17}O$, $\delta^{18}O$, and $^{17}\Delta$ is 0.017 ‰, 0.030‰, and 6 per meg, respectively.

$\delta O_2/Ar$ was obtained by peak jumping; a sequential measurement of m/z '32' and '40' in the same collector (the idle and integration times were 20 and 4 s, respectively, following Barkan & Luz 2003) prior to isotope ratio analysis. $\delta O_2/Ar$ is expressed in the standard δ-notation and calculated as $\delta O_2/Ar$ (‰) = $[(32/40)_{sample}/(32/40)_{standard}-1]10^3$. The long-term precision (1-σ standard deviation) of routine measurements of atmospheric air was better than 5‰.

To verify the sample purity after chromatographic separation, we have also included measurement of m/z '28' during peak jumping. Similar to Luz & Barkan (2003) and Abe & Yoshida (2003), we found that the values of $\delta^{17}O$ and $\delta^{18}O$ depend on variations in the O_2/Ar, presumably due to interference with the ion source of the mass spectrometer. Thus applying a correction is necessary for high precision work. We have calculated these based on dependencies of $\delta^{17}O$ and $\delta^{18}O$ on $\delta O_2/Ar$, derived from measurements of aliquots of pure O_2 with added different amounts of Ar.

To minimize the influence of Ar and for obtaining of more precise results, we use a working O_2-Ar reference mixture from pure gases (>99.999%) with the proportion of O_2/Ar ~20:1, similar to the O_2-Ar solubility ratio in surface water (Benson & Krause 1984, Krause & Benson 1989, Barkan & Luz 2003). The integrity of the standard was checked regularly by measuring samples of air O_2. In addition, for every set of samples (one set representing one trip to the reservoir) three samples of atmospheric air O_2 were prepared and measured against the same aliquot of working reference gas mixture as used for the sample set.

Biogeosciences Discuss., doi:10.5194/bg-2016-49, 2016
Manuscript under review for journal Biogeosciences
Published: 17 February 2016

2.4 Gross and net production calculations

Aquatic primary production (PP), the synthesis of organic compounds from aqueous carbon-containing species, is distinguished as gross production (GP) and net production (NP). The GP represents the total carbon fixed by primary producers, and the NP represents the carbon available to the heterotrophic community. The NP is therefore the difference between GP and community respiration (R) and corresponds to the overall metabolic balance of an ecosystem. NP can be positive or negative. NP is positive when GP exceeds R and the ecosystem may export or store organic C. The value is negative when R exceeds GP and the ecosystem respires more organic C than was able to produce. Both GP and NP are terms of fundamental interest in carbon cycle studies.

To quantify gross production rates from $^{17}\Delta$ values, a simple box model may be applied; mixed layer GP is assumed at steady state with respect to $^{17}\Delta$ and O_2 concentrations, and vertical mixing is neglected (Luz & Barkan, 2000). We use the following equation for estimating gross oxygen production (GOP):

$$GOP = KC_o(^{17}\Delta - ^{17}\Delta_{eq})/(^{17}\Delta_{bio} - ^{17}\Delta), \quad (2)$$

where Co is O_2 solubility (Benson & Krause 1984) and K is piston velocity (the coefficient for gas-exchange; Crusius et al. 2003, Wanninkhof et al. 2009). K was calculated from daily wind speed and then averaged over 1 week according to Wanninkhof et al. (1987) and Vachon and Prairie (2013), based on studies of gas transfer velocities in lakes of comparable sizes to Feitsui Reservoir. $^{17}\Delta_{eq}$ is the air-water equilibrium, deviating from zero due to isotopic fractionation during O_2 invasion, and $^{17}\Delta_{bio}$ is the value of biologically produced O_2 (i.e., $^{17}\Delta$ of water).

^{14}C production estimates were also derived. In summary, bottles were incubated for approximately 2~3 hours and PB-I model was used to calculate primary production over 24 hours, depending on the daily solar irradiance. The ^{14}C rates reflect gross C production and are integrated for the euphotic zone. Detailed description of methodology for ^{14}C light incubations experiments is provided in Shiah et al. (1996).

To estimate the net oxygen production (NOP) rates, we have used the $\delta O_2/Ar$ measurements, following the 'biological O_2 supersaturation' concept for net photosynthetic production. Because the physical properties of O_2 and Ar are similar, and Ar has no biological sources and sinks, measurements of Ar supersaturation may be used to remove physical contributions to O_2 supersaturations (Craig & Hayward 1987, Spitzer & Jenkins 1989). Since the early works on $^{17}\Delta$ of dissolved O_2 (e.g., Luz et al. 2002, Hendricks et al. 2004), measurements of $\delta O_2/Ar$ have become a standard routine. Biological supersaturation may be calculated as

Biogeosciences Discuss., doi:10.5194/bg-2016-49, 2016
Manuscript under review for journal Biogeosciences
Published: 17 February 2016

$$([O_2]/[O_2]_{eq})_{bio} = (O_2/Ar)_{measured}/(O_2)/(Ar)_{eq} = \delta[(O_2/Ar)_{measured}]+1/\delta[(O_2/Ar)_{eq}]+1, \quad (3)$$

where $[O_2]$ is the observed concentration, $[O_2]_{eq}$ is equilibrium solubility value at in situ temperature and $([O_2]/[O_2]_{eq})bio$ stands for the 'biological O_2 saturation'. Following the above and the assumption that mixed layer is at steady state, NOP can be calculated following Luz et al. (2002):

$$NOP = KC_o[([O_2]/[O_2]_{eq})_{bio}-1]. \quad (4)$$

A shortcoming associated with the calculation of PP rates from dissolved O_2 isotopes is that the rates are in O_2 units, instead of C based units, and the conversion between them is not straightforward. To convert between O_2 and C based rates, we follow the common approach presented earlier (e.g., Hendricks et al. 2014, Juranek et al. 2012). GOP from $^{17}\Delta$ is greater than gross C production because it measures total oxygen produced regardless of its fate, such as the fraction of O_2 produced which is linked to Mehler reaction and photorespiration. To scale GOP to gross C production, we account for this fraction following Laws et al. (2000) and apply a photosynthetic quotient (PQ) of 1.2. We convert NOP to a comparable C flux using a PQ of 1.4, for new production (Laws 1991).

3 Results

3.1 Hydrography

Throughout the results section we refer to our monthly sampling dates as MMMYY for convenience. The subtropical Feitsui Reservoir was thermally stratified for the great part of the year, with a distinct seasonal thermocline (Figure 2). In spring permanent stratification developed (APR15), and the lake remained well stratified with a clear shallow epilimnion with temperatures above ~30°C throughout the summer. As of OCT14, when the ambient temperature started to decrease, the surface of the lake gradually cooled and the thermocline deepened until the winter overturn when the stratification completely disappeared. From around JAN15 the lake stayed homothermal at ~17°C for a short period of one to two months, and then again began to stratify as the ambient temperature increased. The mixed layer depth varied with seasons. During the warmer part of the year in JUN14/ JUN15, AUG14, APR15 and MAY2015, the mixed layer was shallow at ~3-5 m deep. In late SEP14 (11 m), OCT14 (23 m), DEC14 (34 m), JAN15 (51 m) and FEB15 (40 m), a defined mixed layer was present. The photic layer depth showed less seasonal variation, with turbidity from phytoplankton or sediment among other lake processes having an effect on the light penetration varying between 17 and 35 m.

Biogeosciences Discuss., doi:10.5194/bg-2016-49, 2016
Manuscript under review for journal Biogeosciences
Published: 17 February 2016

Chl *a* concentration was high from JUN14 to SEP14, with a clear subsurface maximum below the mixed layer at ~10 m, averaging to 15 mg m^{-3} and occasionally above 20 mg m^{-3}. In late SEP14, the Chl *a* maximum shifted to the surface. No clear maximum was observed in OCT14 when Chl *a* concentration was rather uniform throughout the mixed layer of average ~8 mg m^{-3} in the upper 23 m. From DEC14 to FEB15, Chl *a* concentration remained low at ~3 mg m^{-3}, with the exception of a small episodic subsurface maximum of ~5 mg m^{-3} at 8 m in JAN15. As of FEB15 and MAR15, Chl *a* concentration showed an increase, first at the surface averaging ~5 mg m^{-3}, later a subsurface maximum was formed at 12 m of ~8 mg m^{-3}, respectively. A short episodic decrease in Chl *a* was seen in APR15, a result likely to be due to untypical cooler ambient temperature and frequent precipitation. In MAY15, Chl *a* concentration started to increase with a high subsurface maximum of >10 mg m^{-3} at 15 m.

The upper water column was largely supersaturated in dissolved oxygen (>120%) between MAY14-JUL14 and MAY15-JUL15, with maximal dissolved O_2 saturation above 300% in the epilimnion in JUL14. In AUG14, the concentration of dissolved O_2 near and above the saturation level became confided to the thermocline in the upper 10 m. The water below usually stayed undersaturated, with O_2 saturation low at ~50%. In late AUG14 and SEP14, the midwater was at saturation. In OCT14 and NOV14, dissolved O_2 concentration was lowest, with a mixed layer averaged saturation of 80% and a shallow undersaturated hypolimnion. As of DEC14 the deep mixed layer and weak thermocline facilitated more homogenous distribution of dissolved O_2 concentration throughout the water column.

3.2 Isotopic composition of water

In addition to dissolved O_2, we have measured the isotopic composition of water in the Feitsui Reservoir (Figure 3). The isotopic composition of water varied in both δ^D and $\delta^{18}O$ seasonally and vertically. Overall, the variation of $\delta^{18}O$ was smaller than that of δ^D, varying between -6.5 and -5.3‰ in $\delta^{18}O$ and between -37.1 and -25.4‰ in δ^D. The general pattern for both, δ^D and $\delta^{18}O$, showed more depleted values during autumn, followed by gradual enrichment throughout the winter, spring and early summer. The $^{17}\Delta$ values for selected waters from JUL14 and AUG14 were determined, which gave the biological end-member ($^{17}\Delta_{bio}$) of 246±11 per meg used for GP calculations presented below.

3.3 The $^{17}\Delta$

The schematics of $^{17}\Delta$ transport and variation are summarized in Figure 4. In Feitsui Reservoir, the $^{17}\Delta$ signal of dissolved O_2 varied with depth and season (Figure 5). The overall range of the $^{17}\Delta$ values measured varied between the maximum of 186 per meg in late AUG14 and JUL15 and minimum of 19 per meg in JUN14. The annual mean $^{17}\Delta$ at the surface (1 m) was 58±10 per meg and remained constant throughout the year, with the exception of late SEP14 and JUL15, when the surface values were higher at 91 and 71 per meg, respectively. On both occasions we observed changes in Chl *a*; in SEP14 the high

Biogeosciences Discuss., doi:10.5194/bg-2016-49, 2016
Manuscript under review for journal Biogeosciences
Published: 17 February 2016

surface $^{17}\Delta$ coincided with an episodic shift in Chl *a* maximum to the surface and in JUL15 we also observed high Chl *a* concentration near the surface.

During months with persistent thermal stratification in the reservoir, the $^{17}\Delta$ followed a similar vertical pattern, with distinct $^{17}\Delta$ values. From JUN14 to early SEP14, when the mixed layer was very shallow (~3-5 m), the $^{17}\Delta$ value accumulated below, with a peak of >150 per meg observed typically at ~10-15 m depth. Below the thermocline (50 m), the $^{17}\Delta$ was low in AUG14 and SEP14 with $^{17}\Delta$ typical of surface water. In late SEP14 and OCT14 when the mixed layer deepened, the subsurface $^{17}\Delta$ remained high, with the values of 182 and 137 per meg at 20 and 30 m, respectively. By DEC14 the thermal stratification nearly disappeared, facilitating gas exchange throughout the water column with rather uniform $^{17}\Delta$ values of 55±5 per meg. The $^{17}\Delta$ values were relatively low and less variable through the winter months. By APR15 the onset of thermal stratification allowed for $^{17}\Delta$ to increase below the mixed layer, where we observed a small peak of 99 per meg at 10 m. The $^{17}\Delta$ signal increased throughout MAY15, and in JUN15 and JUL15 the accumulated $^{17}\Delta$ signal was high at 10-30 m, averaging 157±35 per meg. In JUL15, the $^{17}\Delta$ followed a similar pattern as the previous year in AUG14 and SEP14, with high $^{17}\Delta$ values in the subsurface and deep regions and with $^{17}\Delta$ of surface water at 30 m. Although samples from regions below 50 m and 70 m were limited due to insufficient amount of gas for isotope analysis, the $^{17}\Delta$ values increased clearly towards the bottom of the hypolimnion. The $^{17}\Delta$ values were particularly high at 70 m in late AUG14, SEP14, and JUL15, measuring 133, 131 and 165 per meg, respectively.

The near-surface $^{17}\Delta$ value represents a balance between O_2 produced photosynthetically, which tends to increase the $^{17}\Delta$, and that from gaseous exchange with atmospheric O_2, which reduces the $^{17}\Delta$ value. The nearly constant surface $^{17}\Delta$ value throughout the year suggests that the balance of these processes does not typically vary with seasons. In late SEP14 and in JUL15, the surface $^{17}\Delta$ values were 33 and 13 per meg higher, respectively, than the annual mean, indicating additional input from photosynthesis. Further analysis showed that in both cases, the samples were taken withing a few days after typhoon occurrences. The resulting elevated $^{17}\Delta$ is likely to be a consequence of nutrient enrichment caused by typhoons, mediating enhanced vertical mixing and hence photosynthesis (see Sect. 4.3).

The high subsurface $^{17}\Delta$ may be primarily attributed to the decreasing importance of gas exchange with depth. This is particularly characteristic of the warmer months, with strong thermal stratification and primary producers confined to the thermocline where conditions are optimal for phytoplankton growth, representing a compromise between light, temperature, and nutrient availability. Low $^{17}\Delta$ values, typical of near-surface $^{17}\Delta$, observed below the thermocline may be explained by the entrainment of dissolved O_2 from the epilimnion. Minimal $^{17}\Delta$ values associated with increase in dissolved O_2 concentrations are indicative of O_2 entrainment from the atmosphere, due to lake processes such as seiches or external

Biogeosciences Discuss., doi:10.5194/bg-2016-49, 2016
Manuscript under review for journal Biogeosciences
Published: 17 February 2016

forcing and episodic events such as storms, heavy precipitation events and typhoons. Increase in the $^{17}\Delta$ towards the bottom of the lake (90 m samples) was observed during all seasons, originating likely from the transport of enhanced $^{17}\Delta$ values from the upper part of the water column and any photosyntheticallty induced changes to the signal before it reached the bottom. These samples however contained only small amounts of O_2 (saturation less than ~50%), and therefore it is possible that minor photosynthetic contributions could significantly increase the $^{17}\Delta$ values.

3.4 Gross and net production

GP rates, NP rates and the NP/GP ratio obtained from $^{17}\Delta$ are summarized in Table 1. Overall, the $^{17}\Delta$ GP rates varied between 47 and 900 mg C m^{-2} d^{-1}. The general pattern showed lower $^{17}\Delta$ GP rates for the warmer months, from JUN14 to early SEP14 and between APR15 and JUN15, when the $^{17}\Delta$ GP averaged 215±93 mg C m^{-2} d^{-1}. This represents the minimum $^{17}\Delta$ GP for this period, because the mixed layer is shallower than the euphotic zone and therefore some production also took place below the mixed layer, which is not considered in the current model. Conversely, higher GP rates were measured from OCT14 to JAN15, averaging 523±66 mg C m^{-2} d^{-1}. This can be considered as the maximum production because the mixed layer is deeper than the euphotic zone. The GP was unusually low in FEB15 at 47 mg C m^{-2} d^{-1}, and high during late SEP14 and JUL15, at 894 and 900 mg C m^{-2} d^{-1}, respectively. While the low FEB15 GP rates are rather difficult to explain, due to the intrinsic relationship between the multiple deterministic and stochastic factors that control the PP, the high GP rates in SEP14 and JUL15 coincide with typhoon events affecting the area of the Feitsui Reservoir (see Sect. 4.3). Overall, the NP varied between 8 and 215 mg C m^{-2} d^{-1}.. The NP was lowest in JUN14 and between FEB15 and JUN15 averaging 23±16 mg C m^{-2} d^{-1}.. Highest NP rates were recorded in late SEP14, JAN15 and JUL15 yielding 154, 165 and 215 mg C m^{-2} d^{-1}., respectively. The NP/GP ratio varied slightly throughout our study period between 0.02 and 0.36 but showed positive values, implying the reservoir remained net autotrophic in the mixed layer.

Using the GP and NP rates measured in our study, we estimated the annual C production in the Feitsui Reservoir. Excluding the measurements obtained during episodic typhoon events (late SEP14 and JUL15), the average annual GP amounted to 104 g C m^{-2} $year^{-1}$ and the average annual NP was 22 g C m^{-2} $year^{-1}$. Taking into consideration typhoon events, the respective rates would increase by approximately 30%. For comparison, based on a model study by Lewis (2011), the global average annual production per unit area for a lake is 200 g C m^{-2} $year^{-1}$ for GP and 160 g C m^{-2} $year^{-1}$ for NP. Our estimates agree moderately well with these values, and both GP and NP are lower than the global averages, most likely due to less optimal natural conditions in the reservoir than applied in the model. The production rates obtained during our study period suggest that the Feitsui Reservoir is presently in mesotrophic to oligotrophic state.

Biogeosciences Discuss., doi:10.5194/bg-2016-49, 2016
Manuscript under review for journal Biogeosciences
Published: 17 February 2016

4 Discussion

4.1 Uncertainties in PP rates

It is important to consider the uncertainties associated with the estimates of the production rates from the $^{17}\Delta$ method. Luz and Barkan (2000) demonstrated that GP in the mixed layer could be determined from the measurements of $^{17}\Delta$ of dissolved O_2 using a steady state mixed layer oxygen budget model which allows for estimation of integrated gross productivity in the mixed layer over the life time of O_2 (approximately 1 to 2 weeks). Although this model lacks terms for advection and vertical mixing, the effect of these simplifications on $^{17}\Delta$ is comparatively negligible (Emerson et al. 1997). It is important to note that this approach may underestimate GP on occasions when the euphotic zone is deeper than the mixed layer since the calculation accounts for GP in the mixed layer only. In particular, this could affect the estimates in summer the most, when the photic layer is typically about 4 times deeper than the mixed layer in the Feitsui Reservoir. As a result, our $^{17}\Delta$ GP estimates compare well with the estimates from ^{14}C bottle incubation in wintertime whereas the $^{17}\Delta$ GP values are significantly lower in summertime.

The key parameter to constrain the GP and NP rates via the $^{17}\Delta$ model and $\delta O_2/Ar$ approach is the gas exchange rate between the mixed layer and the atmosphere. Presently this is best achieved by parameterization of wind speeds, which is commonly used in models with several empirical relationships between the wind speed and gas exchange rate (e.g. Clark et al. 1995, Ho et al. 2006, Wanninkhof et al. 2009). Yet parameterization of wind speeds does not come without inaccuracies. While in most of the oceanic studies, the error associated with the parameterization is attributed to the accuracy of wind speed measurements and the relationship between the wind speed and gas exchange rate at very high or low wind speed conditions (Wanninkhof 1992). In freshwater systems, factors such as lake size and ecosystem heterogeneity present another important factor (Vachon and Prairie 2013) and should be taken into consideration when choosing an appropriate parameterization.

Apart from $^{17}\Delta$ measured in samples, $^{17}\Delta_{eq}$ and $^{17}\Delta_{bio}$ are important constituents of the $^{17}\Delta$ model. $^{17}\Delta_{eq}$ is rather well established and can be determined experimentally, typically by bubbling or stirring method. We measured $^{17}\Delta_{eq}$ using a bubbling method to be 9±3 per meg. $^{17}\Delta_{bio}$ reflects the $^{17}\Delta$ of water, which is considered uniform in seawater but differs geographically between water sources. Over the period of the study we have measured the $\delta^{18}O$ of water in Feitsui Reservoir with an annual mean -6.03±0.22‰ vs. VSMOW (-29.21‰ vs. air). Measurements of $^{17}\Delta$ of reservoir water yielded 246±11 meg vs. air O_2 for $^{17}\Delta$bio. For comparison, Luz and Barkan (2000) determined $^{17}\Delta_{bio}$ in Lake Kinneret to be 159 per meg.

Estimating the net production is less complicated, since the model only requires the coefficient for gas exchange and a term describing 'biological supersaturation.' The later term can be constrained by the $\delta O_2/Ar$ measurements from flask samples or

Biogeosciences Discuss., doi:10.5194/bg-2016-49, 2016
Manuscript under review for journal Biogeosciences
Published: 17 February 2016

determined in situ using a sensor for dissolved O_2 supersaturation, although the accuracy of the later is inferior and is less suitable for this purpose.

Combining $^{17}\Delta$ and $\delta Ar/O_2$ measurements we can get the net to gross production ratio (NP/GP) which is equivalent to an export ratio (Laws et al. 2000) describing the capacity of an ecosystem to export C. The NP/GP ratio can be far better constrained than the GP on its own, since it is independent of the gas exchange rate and the uncertainty in the ratio only depends on the error in the measurement of $^{17}\Delta$ and δO_2 /Ar.

4.2 Comparisons between $^{17}\Delta$ GP and ^{14}C GP rates

While both methods aim to evaluate the natural GP rates, direct comparisons between estimates from the $^{17}\Delta$ method and from the ^{14}C bottle incubations are impractical because of the principal differences in the methodologies (in situ vs. in vitro). Each method provides rates integrated over different spatial and temporal scales, and clearly methodological biases are associated with either of the approaches. A number of studies have addressed the $^{17}\Delta$ GP/^{14}C GP in the ocean, but the ratios were found to vary significantly from 2.2 (Quay et al. 2010) to 8.2±4.0 (Stanley et al. 2010; see also Juranek & Quay 2013 for an extensive review). The variability in the ratios remains a conundrum. Overall, the $^{17}\Delta$ GP method showed a tendency to yield higher production rates. The factors responsible for the variability in $^{17}\Delta$ GP/^{14}C GP have however yet to be properly identified, before the gross O_2 production and carbon fixation can be properly linked.

The comparison between the $^{17}\Delta$ GP and the ^{14}C GP rates (Table 1 and Figure 6) shows that both production rates are on the same order of magnitude, with the long-term $^{17}\Delta$ GP/^{14}C GP ratio being 1±0.8. This is in close agreement with the initial study by Luz & Barkan (2000) who demonstrated near equivalence of gross production rates obtained from incubation-dependent and incubation-independent methods from Lake Kinneret. Presumably, near 1 $^{17}\Delta$ GP/^{14}C GP ratios are characteristic of systems with shallow mixed-layer and rapid O_2 turnover (up to 1 week), such as subtropical reservoirs in general, including the Feitsui Reservoir. Moreover, our results showed less variation in the overall $^{17}\Delta$ GP rates throughout the year and generally lower values than ^{14}C GP which could be attributed to the integration on which each method operates The disparity between the $^{17}\Delta$ GP and ^{14}C GP rates from AUG14 and early SEP14 could be explained by the shallow summer mixed layer where $^{17}\Delta$ GP rates are minimal. Conversely, it could also be that the ^{14}C GP is overestimating the production rates particularly during this period, when algal blooms are more likely to occur. This highlights one of the key assets of the $^{17}\Delta$ GP method, which in principle is not significantly affected by small-scale short-term events. Onwards DEC14 the $^{17}\Delta$ GP and ^{14}C GP can be considered to agree reasonably well.

4.3 Typhoon effects

Biogeosciences Discuss., doi:10.5194/bg-2016-49, 2016
Manuscript under review for journal Biogeosciences
Published: 17 February 2016

Passing of tropical cyclones had been documented to cause entrainment and upwelling or 'atmospheric pumping,' injecting nutrients into the mixed layer which may significantly elevate PP. In the South China Sea, Lin et al. (2003) reported that the occurrence of only a moderate cyclone led to a 30-fold increase in the concentration of surface Chl *a*. Ko et al. (2015) studied the phytoplankton responses to typhoons in the Feitsui Reservoir and found a twofold increase in the phytoplankton level during typhoon periods. The effect of typhoons on ecosystems is however complex and difficult to document properly because of their sporadic occurrence. Although our data is limited to draw solid conclusions, we briefly discuss our results in context to typhoon events.

Two typhoons closely affected the north-eastern Taiwan and the Feitsui Reservoir during our study period. Typhoon Fung Wong hit Taiwan on the 22nd of September 2014 and typhoon Chan Hom on the 10th of July 2015, 1 and 4 days before the sample collection, respectively. Post-typhoon sampling occasions are indicated in Table 1. On both occasions, we found a considerable increase in the GP in the mixed layer (897±4 mg C m^{-2} d^{-1}), representing a 3-fold increase in the GP rates obtained otherwise (Figure 6). This corresponds to 13 and 33 per meg increase in surface $^{17}\Delta$. However, short episodic events of high production are normally expected to average out by the lower background $^{17}\Delta$ of the mixed layer due to elevated gas exchange with air. It is plausible that if the mixed layer is very shallow and the photosynthetic O_2 production is high, the elevated $^{17}\Delta$ signal would remain for an extended period of time. Alternatively, increased $^{17}\Delta$ values could arise from ventilation from water below the mixed layer or enhanced vertical mixing. Greater K caused by higher wind speeds during a typhoon event could explain the higher GP rates; however, it does not explain the increase in $^{17}\Delta$ signal. Nevertheless it is important to note that these GP rates should be considered as minimum values, because on both occasions the thermocline was situated in the photic zone and therefore some of the production also took place below the mixed layer.

5 Conclusions

In summary, the $^{17}\Delta$ and $\delta O_2/Ar$ values showed strong seasonal and vertical variations, enabling us to monitor the photosynthetic activity versus atmospheric O_2 input in a freshwater system. The $^{17}\Delta$ GP and ^{14}C GP estimates were consistent on the same order of magnitude with the $^{17}\Delta$ GP/^{14}C GP ratio of 1±0.8 throughout the study. Although the interpretation of the results is not straightforward, the combined $^{17}\Delta$ and $\delta Ar/O_2$ tracer offers us a new perspective on studying primary production rates in situ. We encourage the use of this technique to evaluate and improve our understanding of the carbon cycling. Further comparisons between the $^{17}\Delta$ and ^{14}C bottle incubation and any other approaches, are needed on various spatial and temporal scales and in particular in dynamic and scientifically well-constrained environments that could serve as 'natural laboratories', such as the Feitsui Reservoir.

Biogeosciences Discuss., doi:10.5194/bg-2016-49, 2016
Manuscript under review for journal Biogeosciences
Published: 17 February 2016

Acknowledgements

We thank the Taipei Feitsui Reservoir Administration Bureau and the Environmental Ecosystem Laboratory group for assistance with fieldwork and making their data available to us. The authors would like to thank Sasadhar Mahata and Ho Wei Kang for their invaluable technical expertise and insights. The work was supported in part by a MOST grant 101-2628-M-001-001-MY4 to Academia Sinica and Academia Sinica Career Development Award.

References

Abe O. and Yoshida N. 2003. Partial pressure dependency of $^{17}O/^{16}O$ and $^{18}O/^{16}O$ of molecular oxygen in the mass spectrometer. Rapid Commun Mass Spectrom 17(5): 395-400.

Barkan, E., Luz, B., 2003. High-precision measurements of $^{17}O/^{16}O$ and $^{18}O/^{16}O$ of O_2 and O_2/Ar ratio in air. Rapid Commun Mass Spectrom 17, 2809-2814.

Benson B.B., Krause Jr., D.K., 1984. The concentration and isotopic fractionation of oxygen dissolved in freshwater and seawater in equilibrium with the atmosphere. Limnol. Oceanogr. 29(3): 620-632.

Craig H. and Hayward T. 1987. Oxygen Supersaturation in the Ocean: Biological Versus Physical Contributions. Science 235(4785): 199-202. doi: 10.1126/science.235.4785.199

Krause Jr., D.K., Benson B.B., 1989.The solubility and Isotopic Fractionation of Gases in Dilute Aqueous Solution. IIa. Solubilities of the Noble Gases. Journal of Solution Chemistry, 18(9).

Castro-Morales, K., Cassar, N., Shoosmith, D.R., Kaiser, J., 2013. Biological production in the Bellingshausen Sea from oxygen-to-argon ratios and oxygen triple isotopes. Biogeosciences 10, 2273-2291.

Cole, J.J., Prairie, Y.T., Caraco, N.F., McDowell, W.H., Tranvik, L.J., Striegl, R.G., Duarte, C.M., Kortelainen, P., Downing, J.A., Middelburg, J.J., Melack, J., 2007. Plumbing the Global Carbon Cycle: Integrating Inland Waters into the Terrestrial Carbon Budget. Ecosystems 10, 172-185.

Clark, J.F., Schlosser, P., Simpson, H.J., Stute, M., Wanninkhof, R., Ho, D.T., 1995. Relationship between Gas Transfer Velocities and Wind Speeds in The Tidal Hudson River Determined by the Dual Tracer Technique. In B. J¨ahne and E. Monahan (eds.), Air-Water Gas Transfer. AEON Verlag.

Crusius, J., Wanninkhof, R., 2003. Gas exchange at low wind speeds over a lake. Limnology and Oceanography 48, 1010-1017 .

Emerson, S., Quay, P.D., Stump, C., Wilbur, D., Schudlich, R., 1995. Chemical tracers of productivity and respiration in the subtropical Pacific Ocean. Journal of Geophysical Research 100, 15873.

Emerson, S., P. Quay, D. Karl, C. Winn, L. Tupas, and M. Landry, 1997. Experimental determination of the organic carbon flux from open-ocean surface waters, Nature, 389, 951–954.

Hamme, R.C., Cassar, N., Lance, V.P., Vaillancourt, R.D., Bender, M.L., Strutton, P.G., Moore, T.S., DeGrandpre, M.D., Sabine, C.L., Ho, D.T., Hargreaves, B.R., 2012. Dissolved O_2/Ar and other methods reveal rapid changes in productivity during a Lagrangian experiment in the Southern Ocean. Journal of Geophysical Research 117, C00F12.

Harrison W.G. and Harris L.R., 1986. Isotope-dilution and its effects on measurements of nitrogen and phosphorous uptake by oceanic microplankton. Mar. Ecol. Prog. Ser. 27: 253-261.

Hendricks, M.B., Bender, M.L., Barnett, B.A., 2004. Net and gross O_2 production in the southern ocean from measurements of biological O_2 saturation and its triple isotope composition. Deep Sea Research Part I: Oceanographic Research Papers 51, 1541-1561.

Hendricks, M.B., Bender, M.L., Barnett, B.A., Strutton, P., Chavez, F.P., 2005. Triple oxygen isotope composition of dissolved O_2 in the equatorial Pacific: A tracer of mixing, production, and respiration. Journal of Geophysical Research 110, C12021, doi:10.1029/2004JC002735

Ho, D.T., Law, C.S., Smith, M.J., Schlosser, P., Harvey, M., Hill, P., 2006. Measurements of air-sea gas exchange at high wind speeds in the Southern Ocean: Implications for global parameterizations. Geophysical Research Letters 33.

Emerson S., Quay P.D., Stump C., Wilbur D. and Schudlich R. 1995. Chemical tracers of productivity and respiration in the subtropical Pacific Ocean. Jour. Geophys. Res. 100: 15,873-15,887.

Juranek, L.W., Quay, P.D., 2010. Basin-wide photosynthetic production rates in the subtropical and tropical Pacific Ocean determined from dissolved oxygen isotope ratio measurements. Global Biogeochemical Cycles, 24, GB2006, doi:10.1029/2009GB003492.

Juranek, L.W., Quay, P.D., 2013. Using triple isotopes of dissolved oxygen to evaluate global marine productivity. Ann Rev Mar Sci 5, 503-524.

Juranek, L.W., Quay, P.D., Feely, R.A., Lockwood, D., Karl, D.M., Church, M.J., 2012. Biological production in the NE Pacific and its influence on air-sea CO_2 flux: Evidence from dissolved oxygen isotopes and O_2 /Ar. Journal of Geophysical Research 117 .

Ko C.-Y., Lai C.-C., Chen T.-Y., Hsu H.-H., Shiah F.-K. (2015) Typhoon effects on phytoplankton responses in a semi-closed freshwater ecosystem. Marine and Freshwater Research, http://dx.doi.org/10.1071/MF14294

Kuo, J.-T., Wen-Cheng Liu, Ruey-Tyng Lin, Wu-Seng Lung, Ming-Der Yang, Chou-Ping Yang, and Show-Chyuan Chu, 2003. Water quality modeling for the Feitsui Reservoir in northern Taiwan. Journal of the American Water Resource Association 39(4): 671-687.

Kuo, J.T., Wang, Y.Y., Lung, W.S., 2006. A hybrid neural-genetic algorithm for reservoir water quality management. Water Res 40: 1367-1376.

Biogeosciences Discuss., doi:10.5194/bg-2016-49, 2016
Manuscript under review for journal Biogeosciences
Published: 17 February 2016

Laskar A. H., Huang J.-C., Hsu S.-C., Bhattacharya S. K., Wang C.-H. and Liang M.-C. 2014. Stable isotopic composition of near surface atmospheric water vapour and rain-vapour interaction in Taipei, Taiwan. Journal of Hydrology 519: 2091-2100.

Laws, E.A., 1991. Photosynthetic quotients, new production and net community production in the open ocean. Deep-Sea Research I 38 (1), 143–167.

Laws, E.A., Landry, M.R., Barber, R.T., Campbell, L., Dickson, M.L., Marra, J., 2000. Carbon cycling in primary production bottle incubations: inferences from grazing experiments and photosynthetic studies using C-14 and O-18 in the Arabian Sea. Deep-Sea Research II 47 (7–8), 1339–1352.

Lewis, W., 2011. Global primary production of lakes: 19th Baldi Memorial Lecture. Inland Waters 1, 1-28.

Lin, I. 2003 New evidence for enhanced ocean primary production triggered by tropical cyclone. Geophysical Research Letters 30(13).

Luz, B., Barkan, E., Bender, M.L., Thiemens, M.H., Boering, K.A., 1999. Triple-isotope composition of atmospheric oxygen as a tracer of biosphere productivity. Nature, 400.

Luz, B., Barkan, E., Sagi, Y., Yacobi, Y.Z., 2002. Evaluation of community respiratory mechanisms with oxygen isotopes: A case study in Lake Kinneret. Limnology and Oceanography 47, 33-42.

Luz B. and Barkan E. 2000. Assessment of Oceanic Productivity with the Triple-Isotope Composition of Dissolved Oxygen. Science 288: 2028-2031.

Luz, B. and Barkan, E., 2005. The isotopic ratios $^{17}O/^{16}O$ and $^{18}O/_{16}O$ in molecular oxygen and their significance in biogeochemistry. Geochimica et Cosmochimica Acta 69, 1099-1110.

Luz, B. and Barkan, E., 2009. Net and gross oxygen production from O_2 /Ar, $^{17}O/^{16}O$ and $^{18}O/^{16}O$ ratios. Aquatic Microbial Ecology 56, 133-145.

Marra J. (2002) Approaches to the measurement of plankton production. Phytoplankton productivity: carbon assimilation in marine and freshwater ecosystem. P. J. leB. Willams, D.N. Thomas, C.S. Reynolds. Cambridge, Blackwells, 78-108.

Munro, D. R., Quay P.D., Juranek L. W., and Goericke R., 2013. Biological production rates off the Southern California coast estimated from triple O_2 isotopes and O_2 : Ar gas ratios, Limnol. Oceanogr., 58(4): 1312–1328, doi:10.4319/lo.2013.58.4.1312.

Prokopenko, M.G., Pauluis, O.M., Granger, J., Yeung, L.Y., 2011. Exact evaluation of gross photosynthetic production from the oxygen triple-isotope composition of O_2: Implications for the net-to-gross primary production ratios. Geophysical Research Letters 38, L14603.

Quay, P.D., Peacock, C., Björkman, K., Karl, D.M., 2010. Measuring primary production rates in the ocean: Enigmatic results between incubation and non-incubation methods at Station ALOHA. Global Biogeochemical Cycles, 24, GB3014, doi:10.1029/2009GB003665.

Quay, P., J. Stutsman, and T. Steinhoff, 2012. Primary production and carbon export rates across the subpolar N. Atlantic Ocean basin based on triple oxygen isotope and dissolved O_2 and Ar gas measurements, Global Biogeochem. Cycles, 26, GB2003, doi:10.1029/2010GB004003.

Reuer, M. K., Barnett B. A., Bender M. L, Falkowski P. G. and Hendricks M. B., 2007. New estimates of Southern Ocean biological production rates from O_2/Ar ratios and the triple isotope composition of O_2, Deep Sea Res., Part I, 54(6), 951–974, doi:10.1016/j.dsr.2007.02.007.

Sarma, V.V.S.S., Abe, O., Hashimoto, S., Hinuma, A., Saino, T., 2005. Seasonal variations in triple oxygen isotopes and gross oxygen production in the Sagami Bay, central Japan. Limnology and Oceanography 50: 544-552.

Sarma, V.V.S.S., Abe, O., Hinuma, A., Saino T., 2006. Short-term variation of triple oxygen isotopes and gross oxygen production in the Sagami Bay, central Japan. Limnol. Oceanogr. 51(3): 1432-1442.

Sarma, V.V.S.S., Abe, O., Saino, T., 2008. Spatial variations in time-integrated plankton metabolic rates in Sagami Bay using triple oxygen isotopes and O_2:Ar ratios. Limnol. Oceanogr. 53(5): 1776-1783.

Schlitzer R. 2015. Ocean Data View, odv.awi.de.

Spitzer W.S. and Jenkins W.J., 1989. Rates of vertical mixing, gas exchange and new production-estimates from seasonal gas cycles in the upper ocean near Bermuda. J Mar Res 47(1):169-196.

Shiah, F.-K., Gong, G.-C., Liu, K.-K., 1996. Light effects on phytoplankton photosynthetic performance in the southern East China Sea north of Taiwan. Bot. Bull. Acad. Sin. 37: 133-140.

Shiau, J.-T., Wu, F.-C., 2010. A dual active-restrictive approach to incorporating environmental flow targets into existing reservoir operation rules. Water Resources Research 46.

Stanley, R.H.R., Kirkpatrick, J.B., Cassar, N., Barnett, B.A., Bender, M.L., 2010. Net community production and gross primary production rates in the western equatorial Pacific. Global Biogeochemical Cycles, 24, GB4001, doi:10.1029/2009GB003651.

Steeman-Nielsen, E. 1952. The use of radioactive carbon (^{14}C) for measuring organic production in the sea. Journal du Conseil, 18: 117 -140.

Tranvik, L.J., Downing, J.A., Cotner, J.B., Loiselle, S.A., Striegl, R. G., Ballatore, T.J., Dillon, P., Finlay K., Fortino, K., 2009. Lakes and reservoirs as regulators of carbon cycling and climate. Limnol. Oceanogr. 54(6, part 2): 2298-2314.

Vachon, D., Prairie, Y.T., 2013. The ecosystem size and shape dependence of gas transfer velocity versus wind speed relationships in lakes. Canadian Journal of Fisheries and Aquatic Sciences 70: 1757-1764.

Valdespino-Castillo P.M., Merino-Ibarra M., Jimenez-Contreras J., Castillo-Sandoval F.S.,Ramirez-Zierold J.A. 2014. Community metabolism in a deep (stratified) tropical reservoir during a period of high-water fluctuations. Environ. Monit. Assess. 186: 6505-6520.

Biogeosciences Discuss., doi:10.5194/bg-2016-49, 2016
Manuscript under review for journal Biogeosciences
Published: 17 February 2016

Wanninkhof, R., 1992. Relationship between wind speed and gas exchange over the ocean. Journal of Geophysical Research 97, 7373.

Wanninkhof, R., Ledwell, J.R., Broecker, W.S., Hamilton, M., 1987. Gas exchange on Mono Lake and Crowley Lake, California. Journal of Geophysical Research 92, 14567.

Wanninkhof, R., Asher, W.E., Ho, D.T., Sweeney, C., McGillis, W.R., 2009. Advances in quantifying air-sea gas exchange and environmental forcing. Ann. Rev. Mar. Sci. 1: 213-244.

Biogeosciences Discuss., doi:10.5194/bg-2016-49, 2016
Manuscript under review for journal Biogeosciences
Published: 17 February 2016

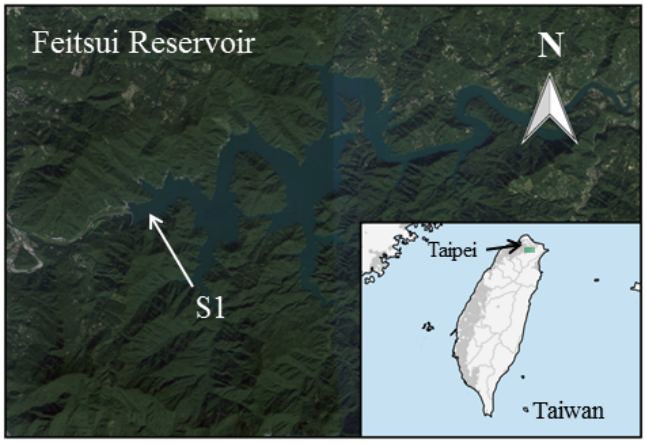

Figure 1. Location of Feitsui Reservoir northern Taiwan. Small green rectangle indicates the enlarged satellite map of the reservoir with the position of the long-term station S1 near the dam indicated.

Biogeosciences Discuss., doi:10.5194/bg-2016-49, 2016
Manuscript under review for journal Biogeosciences
Published: 17 February 2016

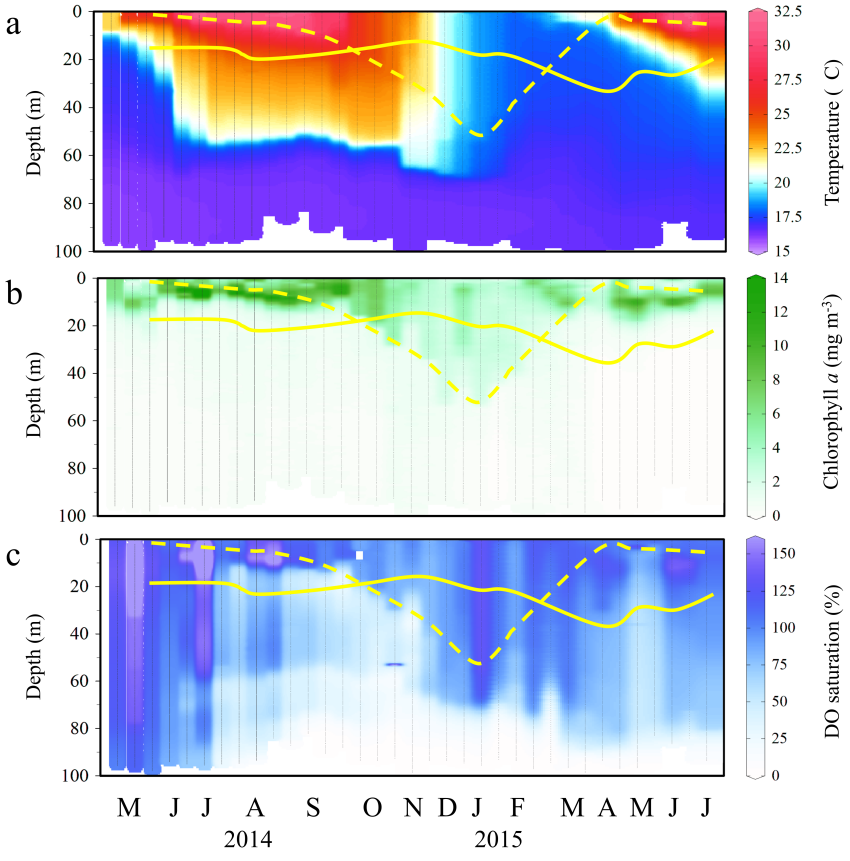

Figure 2. Annual variability in a) temperature (°C), b) chlorophyll a concentration (mg m^{-3}), and c) dissolved oxygen saturation (%) from S1 in the Feitsui Reservoir (S1). Profile data normally collected on weekly basis throughout the warmer months and every two weeks in winter. Solid yellow line indicates the limit of euphotic zone and dashed yellow line the depth of mixed layer.

Biogeosciences Discuss., doi:10.5194/bg-2016-49, 2016
Manuscript under review for journal Biogeosciences
Published: 17 February 2016

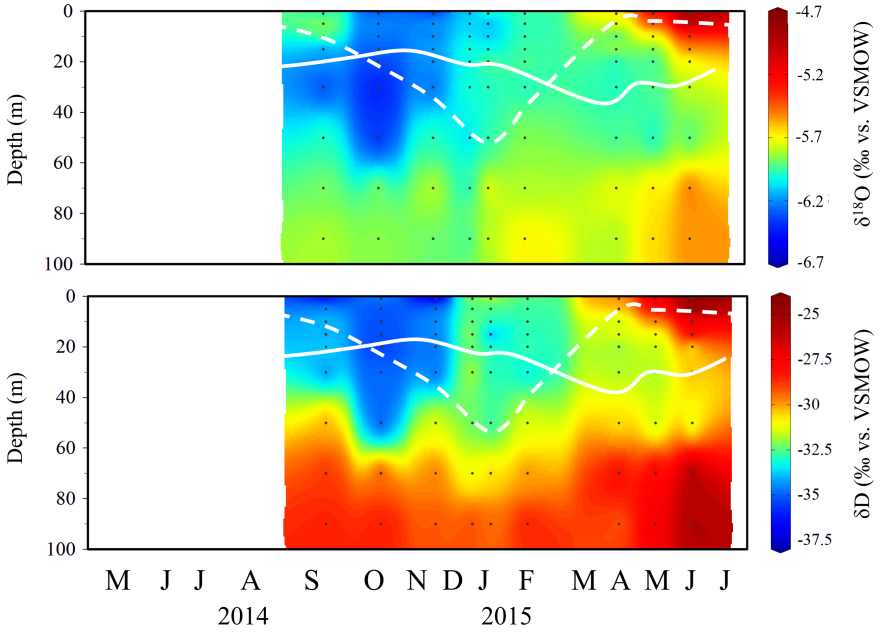

Figure 3. Annual variability in a) $\delta^{18}O$ of water O_2 (‰, vs. VSMOW), and b) δ^{D} (‰, vs. VSMOW). Solid white line indicates the limit of euphotic zone and dashed white line the depth of mixed layer.

Biogeosciences Discuss., doi:10.5194/bg-2016-49, 2016
Manuscript under review for journal Biogeosciences
Published: 17 February 2016

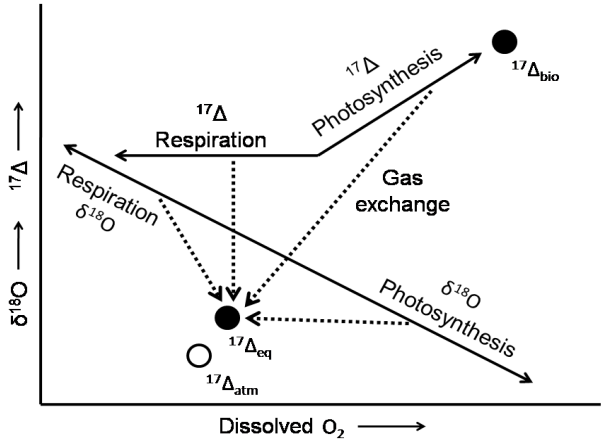

Figure 4. A schematic diagram showing the effects of photosynthesis, respiration and air-water gas exchange on dissolved O_2 concentrations, $\delta^{18}O$ and $^{17}\Delta$. $\delta^{18}O$ changes with all the processes and additionally is also affected by mixing. Because of non-mass dependent processes occurring in the stratosphere, the $^{17}\Delta$ of O_2 in air has a different signal to the O_2 produced biologically where fractionation is mass-dependent. $^{17}\Delta$ increases due to photosynthesis, decreases due to gas exchange but is not affected by respiration. Respiration removes O_2 and decreases the dissolved O_2 concentration but fractionates O_2 isotopes in a mass-dependent way, which does not affect the relative proportion of $\delta^{17}O$ and $\delta^{18}O$ and therefore the $^{17}\Delta$. $^{17}\Delta_{bio}$ is the maximum value of pure biological signal, which amounts to $^{17}\Delta$ of water. The slope of $^{17}\Delta$ increase towards $^{17}\Delta_{bio}$ is the kinetic slope λ for respiration (λ = 0.518). $^{17}\Delta_{eq}$ is the O_2 at air-water equilibrium, which has a small offset from $^{17}\Delta_{atm}$, which is by definition 0, due to fractionation at equilibrium where $\delta^{17}O$ and $\delta^{18}O$ slopes during invasion and evasion follow a slightly different slope to that of respiration.

Biogeosciences Discuss., doi:10.5194/bg-2016-49, 2016
Manuscript under review for journal Biogeosciences
Published: 17 February 2016

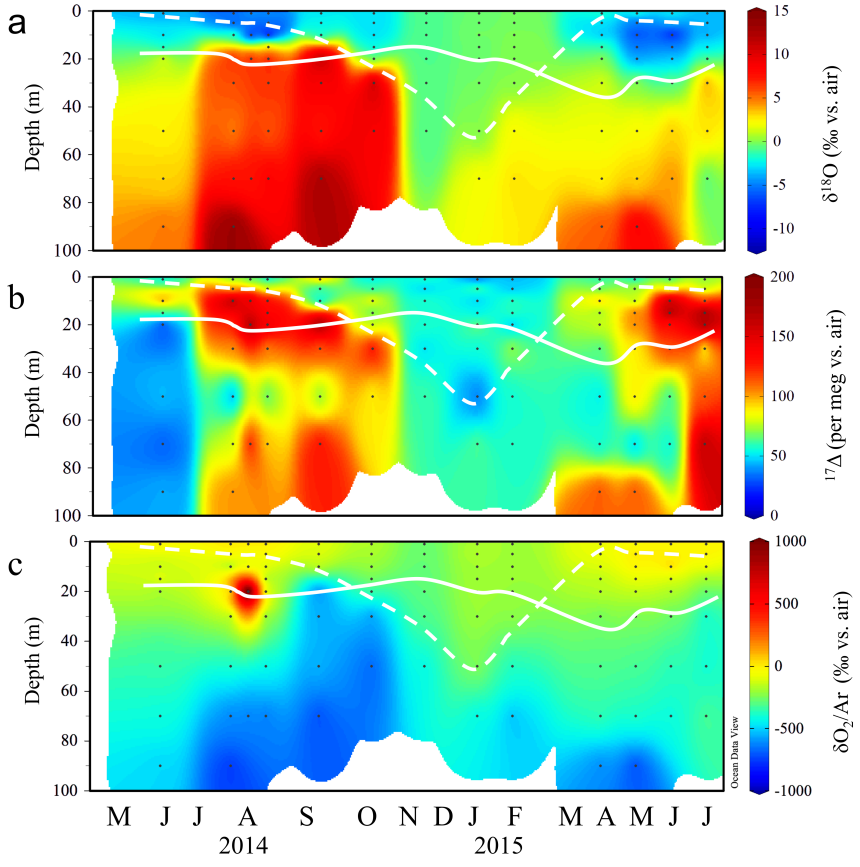

Figure 5. Annual variability in a) $\delta^{18}O$ of dissolved O_2 (‰, vs. air), b) $^{17}\Delta$ (per meg, vs. air) and c) $\delta O_2/Ar$ (‰, vs. air) in Feitsui Reservoir. Solid white line indicates the limit of euphotic zone and dashed white line shows the depth of mixed layer.

Biogeosciences Discuss., doi:10.5194/bg-2016-49, 2016
Manuscript under review for journal Biogeosciences
Published: 17 February 2016

Figure 6.

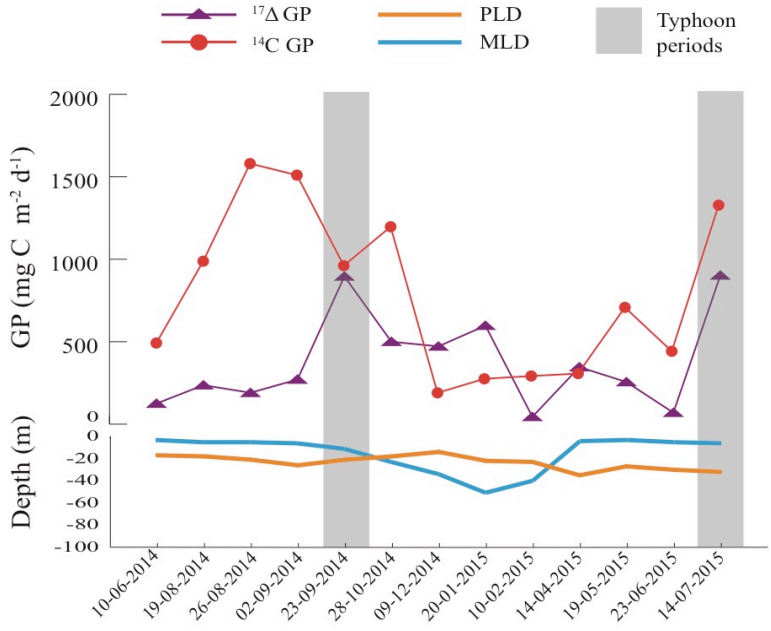

Figure 6. Time series of $^{17}\Delta$ GP and ^{14}C GP rates. PLD and MLD indicate photosynthetic layer depth and mixed layer depth, respectively.

Biogeosciences Discuss., doi:10.5194/bg-2016-49, 2016
Manuscript under review for journal Biogeosciences
Published: 17 February 2016

Biogeosciences Discussions
Open Access
EGU

1

Table 1. Summary of PP rates (mg C m^{-2} d^{-1}) in the Feitsui Reservoir from June 2014 to July 2015. Dates marked with an asterisk indicate post-typhoon sampling days.

Date	Abbrev.	PLD[a] (m)	MLD[b] (m)	T (°C)	O_2 Sat. (%)	δO_2/Ar (‰) vs. air	C_o (mmol m^{-3})	K from U (m day^{-1})	Δ^{17}_{eq}	Δ^{17}_{bio}	Δ^{17}_{mld} [c]	$^{17}\Delta$ GP	NP (δO_2/Ar) (mg C m^{-2} d^{-1})	NP/ GP	^{14}C GP (mg C m^{-2} d^{-1})
10/06/2014	JUN14	14	3	26.7	109.6	-10	249.01	0.20	9	246	57	127	38	0.30	492
19/08/2014	AUG14	11	5	30.5	107.4	35	232.20	0.30	9	246	69	238	83	0.35	988
26/08/2014	AUG14	14	5	30.9	138.2	18	232.20	0.27	9	246	64	192	64	0.34	1580
02/09/2014	SEP14	17	6	31.0	151.4	18	232.20	0.42	9	246	61	272	99	0.36	1510
23/09/2014*	SEP14	13	11	29.2	101.3	-89	240.36	1.12	9	246	66	894	154	0.17	961
28/10/2014	OCT14	26	23	24.8	94.2	-207	258.23	0.58	9	246	67	500	69	0.14	1197
09/12/2014	DEC14	17	34	21.9	79.9	-285	273.24	0.73	9	246	54	472	80	0.17	190
20/01/2015	JAN15	17	51	18.6	134.7	-178	289.89	0.94	9	246	51	597	165	0.28	275
10/02/2014	FEB15	20	40	17.9	85.6	-199	295.85	0.06	9	246	55	47	10	0.22	292
14/04/2015	APR15	10	4	20.8	107.8	-83	278.59	0.45	9	246	60	347	8	0.02	307
19/05/2015	MAY15	14	3	27.8	116.8	-46	244.62	0.42	9	246	56	257	43	0.17	708
23/06/2015	JUN15	14	5	30.8	109.0	-15	232.20	0.09	9	246	68	72	17	0.24	442
14/07/2015*	JUL15	12	6	29.3	108.5	2	240.36	1.04	9	246	72	900	215	0.24	1328

[a] Photic layer depth
[b] Mixed layer depth
[c] Average Δ^{17} in the mixed layer